Fast-tumbling bicelles constructed from native Escherichia coli lipids

Biochimica et Biophysica Acta 1858 (2016) 2097–2105

Contents lists available at ScienceDirect

Biochimica et Biophysica Acta

journal homepage: www.elsevier.com/locate/bbamem

Fast-tumbling bicelles constructed from native *Escherichia coli* lipids

Jobst Liebau [a], Pontus Pettersson [a], Philipp Zuber [a], Candan Ariöz [a,b], Lena Mäler [a,*]

[a] Department of Biochemistry and Biophysics, Stockholm University, SE-106 91 Stockholm, Sweden
[b] Department of Biology and Biological Engineering, Division of Chemical Biology, Chalmers University of Technology, SE-412 96 Gothenburg, Sweden

ARTICLE INFO

Article history:
Received 16 February 2016
Received in revised form 9 June 2016
Accepted 10 June 2016
Available online 15 June 2016

Keywords:
Native lipids
Bicelle
Model-free approach
Dynamics
Diffusion
Inner membrane
Lipid composition

ABSTRACT

Solution-state NMR requires small membrane mimetic systems to allow for acquiring high-resolution data. At the same time these mimetics should faithfully mimic biological membranes. Here we characterized two novel fast-tumbling bicelle systems with lipids from two *Escherichia coli* strains. While strain 1 (AD93WT) contains a characteristic *E. coli* lipid composition, strain 2 (AD93-PE) is not capable of synthesizing the most abundant lipid in *E. coli*, phosphatidylethanolamine. The lipid and acyl chain compositions were characterized by ^{31}P and ^{13}C NMR. Depending on growth temperature and phase, the lipid composition varies substantially, which means that the bicelle composition can be tuned by using lipids from cells grown at different temperatures and growth phases. The hydrodynamic radii of the bicelles were determined from translational diffusion coefficients and NMR spin relaxation was measured to investigate lipid properties in the bicelles. We find that the lipid dynamics are unaffected by variations in lipid composition, suggesting that the bilayer is in a fluid phase under all conditions investigated here. Backbone glycerol carbons are the most rigid positions in all lipids, while head-group carbons and the first carbons of the acyl chain are somewhat more flexible. The flexibility increases down the acyl chain to almost unrestricted motion at its end. Carbons in double bonds and cyclopropane moieties are substantially restricted in their motional freedom. The bicelle systems characterized here are thus found to faithfully mimic *E. coli* inner membranes and are therefore useful for membrane interaction studies of proteins with *E. coli* inner membranes by solution-state NMR.

1. Introduction

Bacterial membranes are complex bilayers of lipids that form a protective barrier for the cell against the fluctuating outer environment. Beyond being a protective, semipermeable barrier, the lipids that constitute membrane bilayers have functional roles [1,2]. It has for example been shown that phosphatidylethanolamine (PE) is required for correct membrane insertion of LacY [3]. Also, PE, phosphatidylglycerol (PG), and cardiolipin (CL) are involved in membrane-related processes like protein translocation and cell growth [1]. Moreover, the lipid bilayer forms the matrix for integral membrane proteins and is sensed by peripheral membrane proteins. For instance, it has recently been shown that the transmembrane protein proteorhodopsin requires lipids of a specific acyl chain length for optimal function [4] and that the peripheral glycosyltransferases MGS [5–7] and WaaG [8] interact specifically with anionic species of the membrane.

The inner membrane of *Escherichia coli* consists mainly of three types of phospholipids: PE (60–80 mol%), PG (15–30 mol%), and CL (5–10 mol%) [2,9,10]. The lipid composition does not vary in response to changes in growth temperature [11,12] but the ratio of CL increases during the stationary phase [13]. Acyl chains can vary in length and degree of unsaturation depending on growth conditions. Under typical growth conditions, 16:0 acyl chains are the most abundant species (~40%) and about 50% of the acyl chains are unsaturated [14,15]. At the onset of the stationary phase a substantial fraction of double bonds is converted into cyclopropanated species, which are believed to increase the physical and chemical stability of cellular membranes [16–18]. PG is a bilayer-forming lipid while PE is not. In the presence of divalent ions, CL can form a hexagonal phase but it is bilayer-prone otherwise [19]. Therefore, *E. coli* inner membranes maintain considerable curvature stress, which is required for cellular viability [15]. The bilayer is maintained in a fluid, lamellar phase by modifications of the acyl chain composition in response to temperature changes [11].

Solution-state NMR methods have contributed to a detailed understanding of protein-membrane interactions. To render experiments interpretable, the size and complexity of biological membranes have to be reduced due to methodological limitations of solution-state NMR. Micelles and bicelles are membrane mimetic systems that are routinely employed to mimic biological membranes in NMR studies

Abbreviations: CL, cardiolipin; DHPC-d_{22}, tail-deuterated 1,2-dihexanoyl-*sn*-glycero-3-phosphocholine; DMPC, 1,2-dimyristoyl-*sn*-glycero-3-phosphocholine; DMPG, 1,2-dimyristoyl-*sn*-glycero-3-phosphoglycerol; NOE, nuclear Overhauser enhancement; PC, phosphatidylcholine; PG, phosphatidylglycerol; PE, phosphatidylethanolamine; TLC, thin layer chromatography.

* Corresponding author.
E-mail address: lena.maler@dbb.su.se (L. Mäler).

http://dx.doi.org/10.1016/j.bbamem.2016.06.008
0005-2736/

[20,21]. Micelles are detergent aggregates that do not form bilayers and have been shown to distort structure and function of some membrane proteins [22–28]. In contrast, bicelles contain a lipid bilayer and therefore they more closely mimic biological membranes as compared to micelles [21,29]. They are thus widely used NMR-accessible membrane mimetics.

Bicelles are characterized by their q-value, which is the molar ratio of lipids to detergent. For q-values in the range 0.25 to 1 small, isotropic bicelles are formed. In an idealized model isotropic bicelles are aggregates in which lipids form a disk-shaped bilayer stabilized by detergents in the rim [30]. For $q < 0.25$ the spatial segregation of detergents and lipids is most likely lost [31,32], while for $q \gg 1$ large bilayer structures are formed, which under appropriate conditions orient in magnetic fields [33–35]. The simplest bicelles consist of a single bilayer-forming lipid type, e.g. 1,2-dimyristoyl-*sn*-glycero-3-phosphocholine (DMPC), and a detergent-like molecule, e.g. 1,2-dihexanoyl-*sn*-glycero-3-phosphocholine (DHPC), which has shorter acyl chains than DMPC [36,37]. In order to emulate specific properties of natural membranes other lipid species can readily be introduced into bicelles. For instance, to simulate the characteristic negative charge of bacterial membranes, fast-tumbling as well as high q-value bicelles have been enriched with anionic lipids such as 1,2-dimyristoyl-*sn*-glycero-3-phosphoglycerol (DMPG) or 1,2-dimyristoyl-*sn*-glycero-3-phosphoserine (DMPS) [38–42]. Using synthetic lipids, up to around 40% DMPG has been introduced into fast-tumbling bicelles with $q = 0.5$. Moreover, bicelles that contain glycolipids abundant in plant membranes can also be produced and it was shown that up to 30% of either mono- or digalactosyl-diacylglycerol could be incorporated into fast-tumbling bicelles while maintaining the bicelle morphology [43]. Finally, the chain length and degree of unsaturation of lipids in bicelles can be varied [4,31,44], also in aligned bicelles with high q-values [45].

It is not possible to prepare fast-tumbling bicelles (with q-values of 0.5 or lower) with high anionic surface charge density or head-group compositions similar to that of *E. coli* of purely synthetic lipids composed of one single type of acyl chain. Therefore, natural lipids extracted directly from *E. coli* provide a means to fine-tune the lipid composition for studies of peptides and proteins in a realistic lipid environment. Here, we present an in-depth analysis of the dynamics and composition of lipids that were extracted from two strains of *E. coli* membranes in small isotropic bicelles. These new types of bicelles are sufficiently small to conduct solution-state NMR experiments while they at the same time provide a natural environment to investigate protein-membrane interactions [7,40,46]. While the inner membrane of strain 1 (AD93WT) has a typical *E. coli* inner membrane composition (~75% PE, 20% PG, 5% CL), strain 2 (AD93-PE) cannot synthesize PE and its inner membrane consists of about 80% PG and 20% CL [15]. The latter construct can be of specific interest when investigating the role of PE in protein-membrane interactions. Moreover, we investigated the effect of growth temperature on the lipid composition and on the dynamic properties of the corresponding lipid mixtures in bicelles.

2. Experimental procedures

2.1. Materials

Tail-deuterated 1,2-dihexanoyl-*sn*-glycero-3-phosphocholine (DHPC-d_{22}) was purchased from Avanti Polar Lipids (Alabaster, AL).

2.2. Purification of lipids from AD93WT and AD93-PE

Lipids were purified from AD93WT and AD93-PE strains according to the protocol described earlier [7,15]. AD93WT and AD93-PE strains were grown at 30 °C from an overnight culture for 24 h in 2× LB with appropriate antibiotics (25 μg/ml kanamycin and 34 μg/ml chloramphenicol for AD93WT and 25 μg/ml kanamycin for AD93-PE) and 20 mM $MgCl_2$ in the case of AD93-PE. Cells were subsequently collected and re-suspended in 20 mM PIPES, 1 mM EDTA, 150 mM NaCl, and 0.0002% NaN_3 buffer at pH 7.4. Lipids were extracted with chloroform:methanol 2:1 (v/v) and were subsequently washed in the aforementioned buffer to remove divalent ions (in particular Mg^{2+}). The chloroform phase was then collected and purified with adsorption chromatography on a silica gel column. Diacylglycerol and fatty acids were eluted with chloroform and phospholipids were subsequently eluted with methanol. All lipid fractions were concentrated to about 20 mg/ml and kept at −20 °C in a 2:1 (v/v) chloroform:methanol solution. Membrane lipid compositions were checked by thin layer chromatography (TLC) using a separation on Silica Gel 60 plates (Merck, Germany) with chloroform/methanol/acetic acid 85:25:10 (v/v/v) as the mobile phase. All lipids were spotted by iodine staining.

2.3. Growth curves

Cell cultures of AD93WT were grown under the above conditions at 20 °C, 30 °C, and 37 °C and AD93-PE cell cultures were grown at 30 °C. For each condition two cell cultures were grown with a delay of 12 h. The OD_{600} of culture 1 was measured in regular intervals during hours 1–12 and 22–33 of the growth cycle. The OD_{600} of culture 2 was measured in regular intervals during hours 13–21 of the growth cycle.

2.4. Bicelle preparation

The two bicelle types analyzed in this study were: 1. AD93WT bicelles made from AD93WT lipid extract and 2. AD93-PE bicelles made from AD93-PE lipid extract. Moreover, lipids were also extracted from AD93WT cells grown at either 20 °C or 37 °C, in addition to cells grown at 30 °C as described above. The bicelles produced from these lipids are referred to as 20 °C or 37 °C AD93WT bicelles. Assuming a typical lipid composition [15] and average length of the acyl chains of 16.5 carbons [11] average molecular weights of 730 g/mol for AD93WT and 880 g/mol for AD93-PE lipids were calculated. Bicelles were prepared by the removal of the chloroform:methanol solvent under a stream of N_2 gas and lipid films were rehydrated in 50 mM of pH 7.4 phosphate buffer in 100% D_2O to obtain a final concentration of 50 mM lipids. Following the addition of 100 mM of DHPC-d_{22} the sample was subjected to three cycles of freezing at −20 °C and thawing at room temperature to yield $q = 0.5$ bicelles. One should note that since up to 10 mM DHPC is free in solution, the effective q-value is always higher [35]. To reference 1H spectra and as an indirect reference for 31P and 13C spectra [47] 50 μM of 4,4-dimethyl-4-silapentane-1-sulfonic acid was added to the sample.

2.5. NMR spectroscopy

2.5.1. Peak assignment and lipid composition

Experiments to assign ^{13}C, ^{1}H, and ^{31}P peaks in AD93WT and AD93-PE bicelle spectra (natural abundance 1D-^{13}C, 1D-^{1}H, 1D-^{31}P, ^{13}C-HSQC, and ^{31}P heteronuclear experiments) were conducted on a Bruker Avance 600 MHz spectrometer equipped with a triple resonance (^{1}H, ^{13}C, ^{31}P) probe-head. ^{31}P and ^{13}C resonance frequencies were 243 MHz and 151 MHz, respectively. Assignments were obtained from standard literature values [48–50]. Moreover, natural abundance 1D-^{13}C and ^{1}H spectra of synthetic PE, PG, and CL dissolved in chloroform aided the assignment. The spectra of the synthetic lipids in chloroform are shown in Fig. S1A (^{1}H) and B (^{13}C) in the Supplementary material. The lipid composition was calculated from peak integrals in ^{31}P spectra. The composition of chain modifications was obtained from peak integrals in ^{13}C spectra. To ensure that differences in relaxation behavior of acyl chain carbons did not influence the peak integrals, the amount of a specific acyl chain modification is reported with respect to the respective peak integral of 30 °C AD93WT bicelles and not relative to the total acyl chain composition. Variations in lipid concentrations were corrected for by multiplying with a concentration factor obtained

from the methyl peak integral (see Example S1 in the Supplementary material).

2.5.2. Translational diffusion

Translational diffusion coefficients were measured on a 600 MHz Bruker Avance spectrometer using a LED-BPP pulse sequence in which the pulsed field gradient was increased in 32 linear steps [51–53]. The ^{1}H spectra were acquired with a spectral width of 12 ppm, 16 scans and a typical 90° pulse length of 8.5 μs. The maximum gradient strength was 50 G/cm, the gradient pulse length 2 ms, the diffusion delay 0.2 s, and the recycling delay 1.5 s. The gradient strengths were calibrated with a 1% H_2O in D_2O and 0.1 mg/ml $GdCl_3$ standard sample. The translational diffusion coefficient was obtained from a fit of the signal attenuation to the Stejskal-Tanner equation [54]. Diffusion coefficients of lipids were measured using ^{1}H acyl chain peaks (protons bound to C3, C4–Cω1, CH_3, C—C═, Δc, and Δt, see Fig. 1 for nomenclature) and corrected for viscosity differences by multiplying with the diffusion coefficient of H_2O [55] and dividing with the diffusion coefficient of trace HDO in the sample.

2.5.3. Dynamics

Natural abundance ^{13}C longitudinal relaxation (T_1) and nuclear Overhauser enhancement (NOE) experiments were conducted on 500 and 700 MHz (^{13}C frequency of 125 MHz and 176 MHz, respectively) Bruker Avance spectrometers for AD93WT and AD93-PE bicelles. Additionally, T_1 experiments were done on a 600 MHz Bruker Avance spectrometer (^{13}C frequency of 151 MHz) for AD93WT bicelles. Inversion recovery experiments with at least 10 delays ranging between 0.05 s and 6 s were acquired to obtain T_1. NOEs were obtained from a 1D experiment by applying 1H irradiation during a 25 s presaturation period and referencing to a spectrum with no presaturation. For 20 °C and 37 °C AD93WT bicelles T_1 inversion recovery experiments were measured on a 500 MHz Bruker Avance spectrometer. The spectral width of the ^{13}C experiments was 200 ppm and a minimum of 2000 scans were acquired. The length of the 90° pulse was typically 9.5 μs (500 MHz), 14.0 μs (600 MHz), and 13.0 μs (700 MHz).

The dynamics of individual ^{13}C—^{1}H bond vectors were analyzed within the framework of the model-free approach [56–60] assuming that the spectral density function can be described by a squared local order parameter, S^2_{loc}, and a local correlation time, τ_{loc}, of the ^{13}C—^{1}H bond vector and a squared lipid order parameter, S^2_{lip}, and a lipid correlation time, τ_{lip}, of the entire lipid [43,61,62]. Moreover, it is assumed that lipid reorientation and ^{13}C—^{1}H bond dynamics occur on distinct timescales. Under these assumptions the spectral density function is given by [63,64]:

$$J(\omega) = \frac{2}{5}\left(\frac{\left(S^2_{loc} - S^2_{loc}S^2_{lip}\right)\tau_{lip}}{1+\omega^2\tau^2_{lip}} + \frac{\left(1-S^2_{loc}\right)\tau_T}{1+\omega^2\tau^2_T}\right) \quad (1)$$

where $\tau_T^{-1} = \tau_{lip}^{-1} + \tau_{loc}^{-1}$. Since R_1 and NOE are expressed in terms of $J(\omega)$ [63] the dynamical parameters can be obtained from fittings to the experimentally determined relaxation parameters that were measured at two or more field strengths. For ^{13}C natural abundance experiments, dipole-dipole relaxation due to the directly attached proton is the dominant relaxation mechanism [63]. Therefore, other effects, like chemical shift anisotropy, were neglected in the description of R_1 and NOE in terms of the spectral density function.

3. Results

3.1. Assignments

The nomenclature of lipid carbon atoms and the structure of the most abundant lipids occurring in *E. coli* are shown in Fig. 1. The peak assignments of AD93WT and AD93-PE bicelle spectra are given in Tables S1 (^{31}P), S2 (^{1}H and ^{13}C) and Fig. S2 (^{1}H and ^{13}C) of the Supplementary material and in Fig. 3 (^{31}P). Note that the glycerol peaks of DHPC largely overlap with the glycerol peaks of all other lipids. Since up to 10 mM [31,65], i.e. 10%, of DHPC is present in the samples as monomers, and thus not bicelle-bound, and in fast exchange with bicelle-bound DHPC, peaks overlapping with DHPC are skewed towards

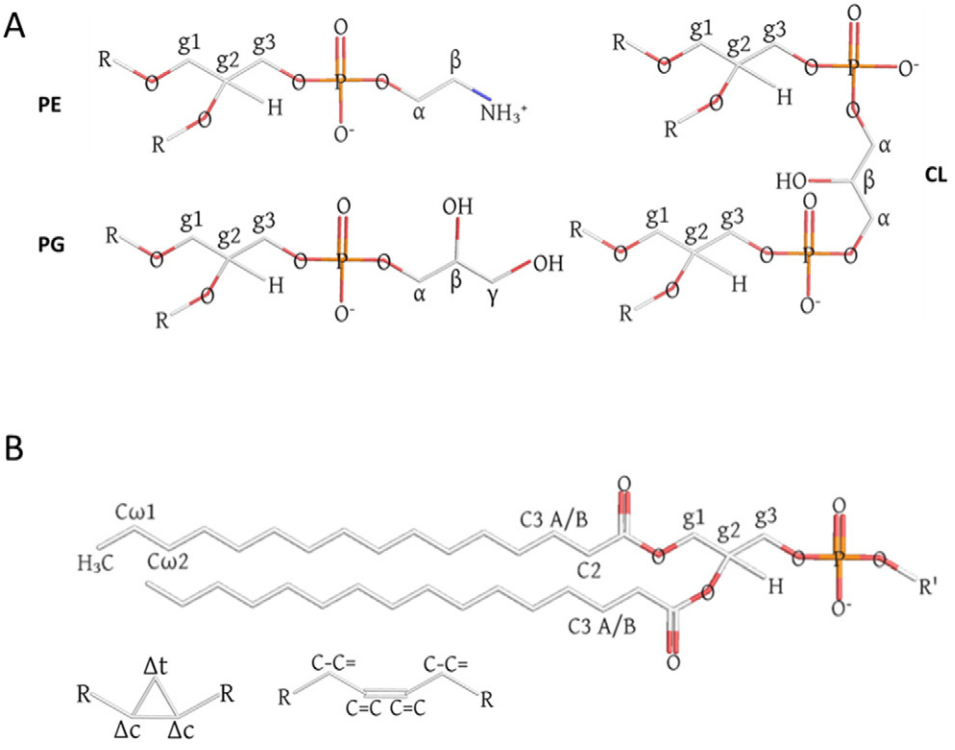

Fig. 1. Nomenclature of lipid carbons: A) head-groups of PE, PG, and CL. B) Saturated acyl chain (top) and two common modifications of lipid acyl chains: cyclopropanation (bottom left) and unsaturation (bottom right).

faster dynamics. Nevertheless, the dominating contributions originate from membrane-bound molecules and a qualitative interpretation of the dynamics of the glycerol backbone carbons is thus feasible within the validity of the model-free approach (see below).

3.2. Growth curves

The growth curves for AD93WT at 20 °C, 30 °C, and 37 °C and for AD93-PE are shown in the Supplementary material, Fig. S3. 30 °C AD93WT reaches the stationary phase after 9 h. The growth behavior at 37 °C of AD93WT is initially the same, but at this temperature AD93WT does not reach the same density as cells grown at 30 °C. At 20 °C, AD93WT grows significantly more slowly and does not reach the highest cell density after 33 h. AD93-PE cells grow more slowly and to a significantly lower density than AD93WT cells grown at the same temperature.

3.3. Lipid composition

The lipid composition of each mixture can readily be obtained by integrating peaks in ^{31}P NMR spectra and the relative composition of acyl chain modifications was obtained from peak integrals in ^{13}C NMR spectra. Cells were harvested after 24 h of growth and the membrane extracts of the AD93WT strain grown at different temperatures and of AD93-PE were analyzed by TLC (Fig. 2). The phospholipid head-group composition was quantified from ^{31}P spectra (Fig. 3) and the lipid composition of AD93WT and AD93-PE bicelles is shown in Table 1. The relative amounts of PE, PG, and CL in bicelles containing AD93WT lipids from *E. coli* grown at 30 °C are characteristic of inner membranes. PE is the major lipid component in AD93WT bicelles and replaced by approximately equal amounts of PG in AD93-PE bicelles. Since PG and PE have different physicochemical features (PG is bilayer prone and anionic, while PE is non-bilayer prone and zwitterionic) (see Fig. 1), the replacement is not a functional one. The lipid composition of bacteria grown at 37 °C was strongly modified as compared to bacteria grown at 30 °C and a substantial increase in anionic lipids, in particular, was observed. The lipid composition of bacteria grown at 20 °C had lower CL and higher PG levels than the lipid mixture of bacteria grown at 30 °C but the ratios of PE to anionic lipids were identical.

Table 2 shows the change in acyl chain composition in 30 °C AD93-PE bicelles, 37 °C and 20 °C AD93WT bicelles relative to 30 °C AD93WT bicelles (for an example of calculation, see Supplementary material). In AD93-PE bicelles the amount of unsaturated fatty acids was higher than in AD93WT bicelles, which was accompanied by a lower amount of cyclopropane moieties. When comparing AD93WT bicelles grown at different temperatures, it was observed that 37 °C AD93WT bicelles had a substantially lower content of double bonds and a larger amount of cyclopropane moieties. Compared to 30 °C AD93WT bicelles 20 °C AD93WT bicelles had a slightly higher content of unsaturated fatty acids and an unchanged amount of cyclopropanated acyl chains.

3.4. Translational diffusion

The translational diffusion coefficients for AD93WT and AD93-PE bicelles were obtained from the analysis of the diffusion rates of acyl chain proton peaks. For both bicelle types the diffusion coefficients were found to be $6.2 \pm 0.8 \times 10^{-11}$ m^2 s^{-1}. Using the Stokes-Einstein equation a hydrodynamic radius of 3.9 ± 0.5 nm is obtained. The diffusion coefficients correspond to what has previously been reported for other fast-tumbling bicelle systems [30]. Typical values for $q = 0.5$ DMPC/DHPC bicelles were found to be around 5×10^{-11} m^2 s^{-1} [44]. While smaller values were determined for bicelles containing 25% PE and 25% PG head-groups (around 4×10^{-11} m^2 s^{-1}) [66,67], higher values were measured for lipids with unsaturations and chain lengths longer than 14 carbons ($6–7 \times 10^{-11}$ m^2 s^{-1}) [4,31,44]. Since *E. coli* lipids are typically 16.5 carbons long and contain a substantial amount of unsaturations [11], the higher diffusion coefficient observed for the bicelles in this study as compared to DMPC/DHPC $q = 0.5$ bicelles is most likely a consequence of the acyl chain composition. The errors were, however, large and we assume that this is due to inaccurate determination of the lipid concentration in different batches, which results in slightly different q-values (lipid to detergent ratios) and thus diffusion coefficients of the bicelles. The head-group region of the 1H spectrum is dominated by DHPC-d_{22} peaks showing elevated diffusion rates due to the presence of monomeric DHPC-d_{22} which is in fast exchange with bicelle-bound DHPC-d_{22}. DHPC-d_{22} peaks almost entirely mask lipid peaks with the exception of the head-group peaks of PG and CL. Due to their low abundancy, these peaks were too weak in AD93WT bicelles to provide reliable results but as they were stronger in AD93-PE bicelles reliable diffusion coefficients could be determined in this case (see Fig. S2A and B). A diffusion coefficient of 6.5×10^{-11} m^2 s^{-1} was observed for those peaks in AD93-PE bicelles, in good agreement with the diffusion coefficients obtained from lipid acyl chains. Therefore, and since all acyl chain carbons show the same diffusion coefficient, we conclude that all lipids partition into the same type of bicelle aggregate.

3.5. Lipid dynamics

In order to analyze the dynamics of individual ^{13}C—^{1}H bond vectors, we measured T_1 and NOE relaxation parameters for AD93WT and AD93-PE bicelles, at least at two magnetic field strengths (for the raw data see Tables S3–S5 in the Supplementary material). We then fitted the data to

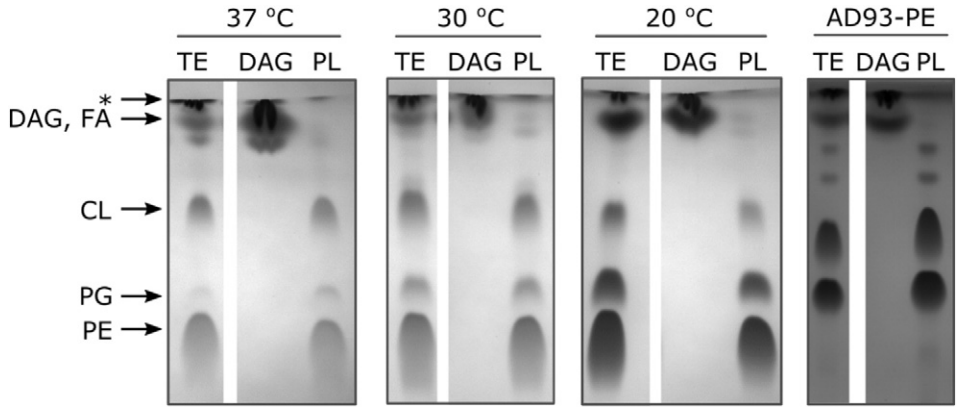

Fig. 2. TLC analysis of the total extract (TE) and the eluted diacylglycerol (DAG) and phospholipid (PL) fractions for the AD93WT and AD93-PE membrane extracts. Lipid extracts were obtained from AD93WT cell cultures grown at 37 °C, 30 °C, and 20 °C and from AD93-PE cell cultures grown at 30 °C. DAG and fatty acids (FA) migrate to the same band level close to the solvent front (*).

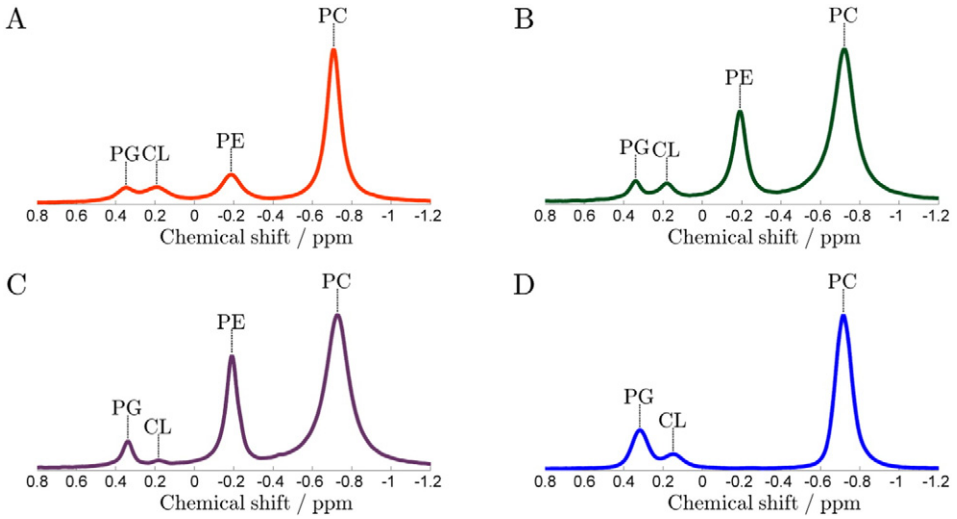

Fig. 3. ^{31}P spectra of A) 37 °C, B) 30 °C, C) 20 °C AD93WT bicelles, and D) AD93-PE bicelles recorded at 25 °C. The phosphate buffer peak is located at 1.8 ppm and not shown in the figures.

a spectral density function (Eq. (1)) and obtained squared local order parameters (S^2_{loc}) and correlation times (τ_{loc}) for the ^{13}C—^{1}H bond vectors and a global squared lipid order parameter (S^2_{lip}) and correlation time (τ_{lip}).

Table 3 shows S^2_{lip} and τ_{lip} for both bicelle types. In the fitting procedure we made the simplifying assumption that all lipid types undergo the same global dynamics, i.e. have similar S^2_{lip} and τ_{lip}, which reduces the number of parameters to be fitted. Since both bicelle systems contain one major lipid component, PE in AD93WT and PG in AD93-PE bicelles, this assumption is reasonable. Moreover, we excluded PC-α, PC-β, and PC-γ peaks from the fitting procedure, since these originate from DHPC-d_{22} molecules that are in fast exchange between a bicelle-bound and a monomeric state. S^2_{lip} and τ_{lip} were found to be similar for AD93WT and AD93-PE bicelles, i.e. the global lipid dynamics were identical for both bicelle systems.

Fig. 4 depicts the dynamic profile of the squared local order parameters of AD93WT and AD93-PE bicelles in the head-groups (Fig. 4A) and in the acyl chain (Fig. 4B), which were obtained by fixing S^2_{lip} and τ_{lip} to the values determined when excluding PC head-group peaks (see also Table S6 in the Supplementary material). The substantial uncertainty is largely due to the difficulty in measuring NOEs, where we assumed a measurement error of 10%. First, it may be noted that the glycerol carbons were the most rigid lipid carbons with S^2_{loc} exceeding 0.7. When comparing the dynamics of carbons in the different types of head-groups it was observed that PC carbons were more dynamic than other types of head-group carbons. In the acyl chains (Fig. 4B) S^2_{loc} was seen to decrease down the chain from the fairly rigid C2 carbons (S^2_{loc} around 0.5) to the highly flexible methyl carbons (S^2_{loc} around 0.05). This trend is interrupted by carbons participating in double bonds and by carbons in the cyclopropane moiety which showed substantially increased rigidity considering that they are typically found at C9 or further down the acyl chain. Finally, C3 carbons in the *sn1* and *sn2* chain experience different magnetic environments and thus show distinct peaks so that their dynamics can be evaluated separately. Here, it was found that C3 carbons undergo identical dynamics. A comparison of the local dynamics of both bicelle types did not show differences in the profiles. The local correlation times (Fig. 4C and D) mirrored the profile of S^2_{loc} and were identical for both bicelle types.

While the model-free approach provides a clear interpretation of the local dynamics in terms of amplitude and rate of motion, and moreover allows for quantification of lipid dynamics that are not directly accessible from NMR data, the inclusion of NOE data as well as the scarcity of data points leads to relatively large errors. However, the trends in R_1 data directly mirror the profile of S^2_{loc} and can be measured with higher reliability. Therefore, they can be used to compare local dynamics without the necessity of a model-free analysis.

In Fig. 5 R_1 relaxation rates of 20 °C, 30 °C, and 37 °C AD93WT bicelles measured at 25 °C are shown. Despite a large degree of variation in the head-group and acyl chain composition (Tables 1 and 2), there are no significant variations in R_1, with the exception of the double bonds of 37 °C AD93WT bicelles for which we suspect that the errors are underestimated. The agreement of R_1 rates at different temperatures indicates that the dynamics of the lipids in the three bicelle systems are the same.

4. Discussion

In this study, we constructed bicelles from the lipid extracts of two different strains of *E. coli* - one having a native *E. coli* lipid composition (AD93WT) and another one that does not synthesize the most abundant *E. coli* lipid PE (AD93-PE). We found that small isotropic bicelles can be made of such lipids and we characterized the diffusion, lipid composition, and dynamics of these bicelles. The dynamics of the individual ^{13}C—^{1}H bond vectors vary along the long axis of the lipid with a rigid glycerol backbone and somewhat more flexible head-groups. The flexibility decreases along the acyl chain but acyl chain modifications lead to a drastic local increase in rigidity.

The lipid composition of *E. coli* strains upon variation of external conditions has previously attracted attention. Wikström et al. [15] analyzed the lipid composition of AD93WT and AD93-PE strains by electronic autoradiography of radio-labeled lipids separated on TLC

Table 1
Lipid head-group composition of bicelles.

Bicelle type	Growth temp./°C	PE	PG	CL
AD93-PE bicelles	30	0%	83%	17%
AD93WT bicelles	37	61%	22%	17%
AD93WT bicelles	30	79%	13%	8%
AD93WT bicelles	20	80%	16%	4%

Table 2
Composition of acyl chain modifications relative to 30 °C AD93WT.

Bicelle type	Growth temp./°C	C=C[a]	C–C=[a]	Δc[a]	Δt[a]
AD93-PE bicelles	30	146%	145%	68%	65%
AD93WT bicelles	37	20%	24%	129%	123%
AD93WT bicelles	20	108%	107%	100%	99%

[a] Peak integrals were normalized for lipid concentration differences by a factor obtained from the peak integral of the methyl peak divided by the peak integral of the methyl peak of 30 °C AD93WT bicelles.

Table 3
S^2_{lip} and τ_{lip} of AD93WT and AD93-PE bicelles measured at 25 °C. Errors are 1 SD.

Bicelle type	S^2_{lip}	τ_{lip}/ns
AD93WT bicelles	0.49 ± 0.05	0.78 ± 0.08
AD93-PE bicelles	0.5 ± 0.1	0.8 ± 0.1

plates to quantify lipid contents. The composition of AD93WT and AD93-PE bicelles found in our study by ^{31}P NMR (Table 1) is in agreement with the results of Wikström et al. [15]. Moreover, in accordance with our study, they observed a decrease in cyclopropane moieties accompanied by an increase in double bonds in the AD93-PE lipid extract as compared to that in AD93WT.

The degree of acyl chain unsaturation increases when bacteria are grown at lower temperatures [68]. This has previously been studied by e.g. Morein et al. [11]. A quantitative comparison of the results is precluded since we only determined changes in acyl chain composition relative to AD93WT, while Morein et al. did not distinguish between cyclopropane moieties and double bonds. For cells grown at 20 °C we find a slight increase in unsaturated fatty acid content, while the opposite is true for cells grown at 37 °C where the amount of unsaturated fatty acids is substantially decreased. These variations are in agreement with the work by Morein et al. [11] even though the present results show more pronounced variations. A reason might be that the *E. coli* strains used in our study (AD93WT and AD93-PE) contain a rather low proportion of unsaturated fatty acids (~40% at 30 °C) [15] compared to *E. coli* K12 used by Morein et al. (~50% at 27 °C) [11] so that a somewhat different response to temperature variations might be expected.

As seen in Table 2 the amount of cyclopropanated species increases with higher growth temperature. Since cyclopropanation mainly proceeds as cells enter the stationary phase and since the 30 °C and 37 °C cultures enter the stationary phase approximately at the same time, it can be speculated that the differing levels of cyclopropanation are a temperature-related effect. It has been reported that elevated amounts of cyclopropanated fatty acids increase the cell's resistance to adverse environmental conditions like high pressure [69–71], osmotic pressure [72,73], acidic conditions [74], or heat shock [69]. Therefore, the observed increase in acyl chain cyclopropanation in bacteria grown at 37 °C could be a reaction to the elevated temperature. On the other hand, the increased levels of unsaturations observed in 20 °C AD93WT and AD93-PE bicelles can be attributed to the fact that cells were harvested after 24 h growth where AD93-PE cells and AD93WT cells grown at 20 °C have not reached the stationary phase, i.e. cyclopropanation occurs only at a basal level.

It is known that *E. coli* does not alter its lipid head-group composition in response to temperature variations [11]. The lipid head-group composition is, however, altered in different stages of the cell's life cycle. In the stationary phase the activity of cardiolipin synthase is upregulated in *E. coli*, a mechanism favorable for viability, and CL is synthesized at the expense of PG [13]. Mutants that only marginally synthesize CL have been reported to grow similar to wildtype [75]. Other reports indicate growth defects [76] and that the viability of such mutants in the stationary phase and under stress conditions is reduced [77,78]. CL levels are upregulated under adverse conditions, like osmotic stress [79,80]. Moreover, CLs form membrane domains, which in turn bind and regulate proteins that are involved in processes like cell division, membrane transport and respiration [81,82] and CL is a versatile substrate for many types of membrane proteins [82].

For cells grown at 20 °C and 30 °C the ratio of PE to anionic lipids is constant but the PG to CL ratio of the 20 °C culture is twice that of the 30 °C culture. Our observation that the composition of anionic lipids in bacteria grown at 20 °C and 30 °C varies can thus be explained by the fact that lipids were harvested at different phases of the growth cycle as evidenced by the growth curves (Fig. S3). The low levels of PE observed in 37 °C AD93WT cells cannot be explained in this way, since PE-levels are independent of the age of the cell culture [83]. It was, however, shown by DeChavigny et al. [84] that the lipid composition of the specific strain used in this study (AD93WT), in contrast to other *E. coli* strains, depends on the growth temperature. Specifically, PE levels of AD93WT are drastically reduced while CL levels are increased when grown at 43 °C. A typical lipid composition is obtained at 30 °C growth temperature [84]. AD93-PE is deficient in PE because it lacks the pss gene product, phosphatidylserine synthase (PssA), which is a crucial enzyme in PE synthesis. AD93WT is derived from AD93-PE in that the deleted gene is reintroduced on a plasmid, the replication of which is temperature sensitive [84]. It has been observed that the activity of PssA in AD93WT drops dramatically in cells grown at 43 °C and cell growth ceases after 4 h. During the growth at this restrictive temperature the amount of CL increases while the amount of PE drops below 30% [84]. It is assumed that CL structurally replaces PE as soon as PE levels are below wildtype level [15,84]. Our results indicate that at 37 °C growth temperature plasmid replication and thus PssA

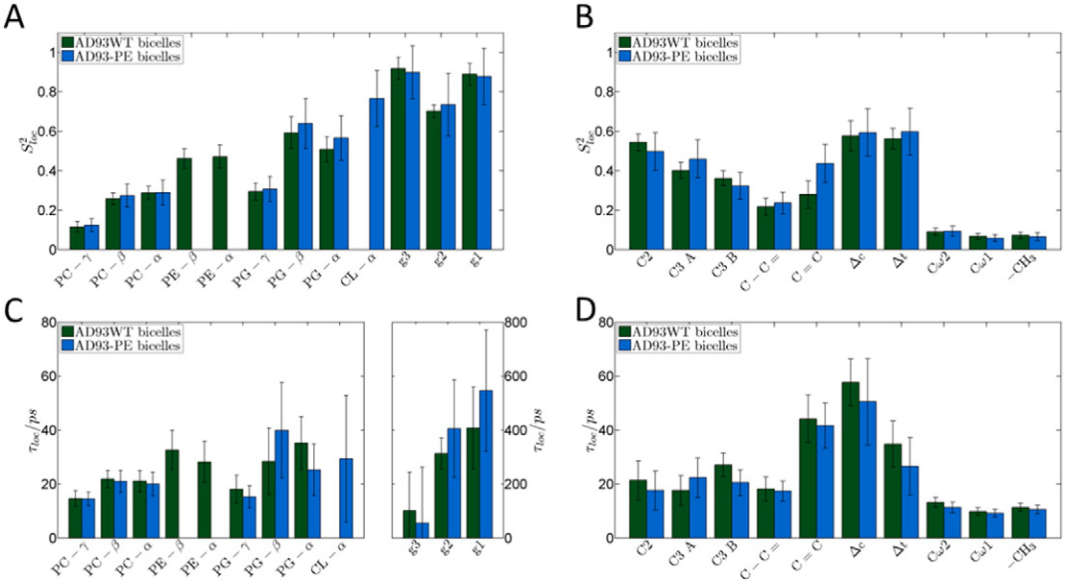

Fig. 4. S^2_{loc} for lipids in AD93WT (green) and AD93-PE (blue) bicelles, measured at 25 °C. Comparison of S^2_{loc} for A) head-group ^{13}C—^{1}H bond vectors and B) acyl chain ^{13}C—^{1}H bond vectors, and τ_{loc} for C) head-group ^{13}C—^{1}H bond vectors and D) acyl chain ^{13}C—^{1}H bond vectors. Errors are 1 SD.

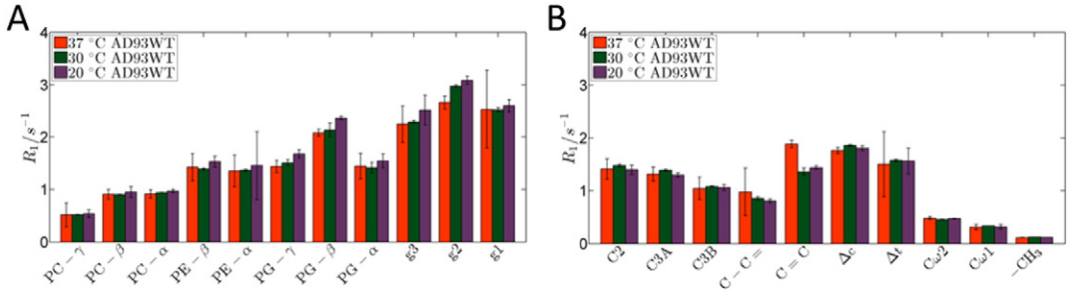

Fig. 5. 13C R_1 relaxation rates for lipids in 37 °C (red), 30 °C (green), and 20 °C (purple) AD93WT bicelles for A) the head-group and B) the acyl chain carbons, measured at 25 °C. Errors are 1 SD.

activity are reduced but not drastically so that a PE level of 60% is obtained. This is below the wildtype level of 80% and it is therefore likely that a structural replacement of PE by CL takes place. In AD93-PE cells increased levels of $MgCl_2$ in the growth medium are required for viability and Mg^{2+} is known to affect the bilayer-forming propensity of CL. While CL in the absence of divalent ions is bilayer forming, the lipid forms a hexagonal phase in their presence, in this way structurally replacing the non-bilayer prone PE. The limited and slow growth of AD93-PE cells shows, however, that addition of Mg^{2+} to the growth medium and the accompanying structural change of CL cannot recover all cellular functions.

The lipid compositions of the different bicelle types studied here are thus a result of strain type, growth temperature, and growth phase. The head-group as well as acyl chain composition can vary drastically in response to variations of these parameters. From a methodological point of view this is a fortunate circumstance, since it means that the lipid composition of the bicelles is, to some degree, tunable. Although not systematically investigated here, it is possible to adjust PE/CL ratios and unsaturation levels by changing the growth temperature. Moreover, PG/CL ratios and cyclopropanation levels are a function of growth phase. Finally, PE can be depleted altogether by using the AD93-PE strain.

The dynamics of individual $^{13}C—^{1}H$ bonds in lipids have previously been investigated in bicelles and vesicles consisting of synthetic lipids [43,85,86]. Ye et al. [43] studied the dynamics of galactolipids in bicelles using the same approach as in this study. The dynamic profile of the acyl chains is in agreement with our findings. In particular, carbons in double bonds show increased rigidity on the ps–ns time-scale and carbons at the far end of the acyl chain are nearly unrestricted in their motion. Interestingly, the head-group dynamics of galactolipids differ from the head-group dynamics of PE and PG. The galactose moieties have squared local order parameters similar to the glycerol backbone while PE and PG head-groups are more flexible. Notably, CL head-group carbons, which are more abundant and thus observable for AD93-PE bicelles, show a high degree of rigidity, similar to galactolipid head-groups. Bulky head-groups are thus severely constrained in their motional freedom while smaller head-groups reorient more freely. The local rigidity of the lipid molecules correlates well with what can be expected for motion around e.g. double bonds or ring structures, and movement of large bulky groups. It is worth pointing out that while the more bulky head-groups and chain modifications lead to more rigid lipid molecules on the ps–ns time-scale, double bonds and other modifications of acyl chains have the overall effect of creating a more fluid membrane due to the overall disordering of acyl chains.

The error analysis of S^2_{loc} indicates large uncertainties for the glycerol carbons and τ_{loc} is on the order of 300–600 ps for g2 and g1. As seen in Table 3, τ_{lip} is about 800 ps, i.e. the model assumption that local and lipid dynamics occur on different timescales is violated for the glycerol carbons. In a thorough analysis of the range of validity of their original model, Lipari and Szabo [59,60] note that the fitting procedure is reliable for local motions in the extreme narrowing limit, where $(\omega_C + \omega_H)$ $\tau_{loc} < 0.5$, corresponding to $\tau_{loc} < 100$ ps for a 700 MHz spectrometer, given that the $S^2_{loc} > 0.01$ and that the global and local motions are separated by at least one order of magnitude. Here, these conditions are met by all but the glycerol carbons. For internal motions outside the extreme narrowing limit and on the same order of magnitude as the global motion, S^2_{loc} is in general overestimated while τ_{loc} is underestimated [60]. Since glycerol correlation times are not in the extreme narrowing limit and similar in magnitude to the overall lipid motion, we conclude that the fitting procedure is unreliable, overestimating S^2_{loc} and underestimating τ_{loc} for the glycerol carbons.

Previous studies suggest that S^2_{lip} ranges between 0.27 and 0.46 depending on lipid type [85]. Lipids in both bicelle types studied here are thus at the upper end of this range and therefore relatively rigid on the ps–ns time-scale (Table 3). Due to the limitations of the fitting procedure described above, it is not obvious whether this observation is significant or not. It is, however, interesting to note that *E. coli* lipids, which are on average more bulky than the saturated, synthetic lipids used in other studies, appear to have more restricted motional behavior, with smaller amplitudes of motion, on the ps–ns timescale compared to saturated lipids. While S^2_{lip} falls in the expected range, τ_{lip} is smaller than previous studies found (1.5–1.9 ns). Investigations of τ_{lip} obtained by the method applied here are, however, scarce [62] and frequently τ_{lip} is not treated as a free fitting parameter [43,86]. It has been suggested that τ_{lip} represents two types of motions: the rotation of a lipid around its long axis and the wobbling of this axis relative to a bilayer normal [62]. The rotational correlation time τ_{rot} of spin-labeled lipids has been investigated by EPR [87,88] using nitroxide (doxyl)-labeled fatty acids [87,88] or doxyl- and TEMPO-labeled phospholipids [86,89]. A pronounced decrease of τ_{rot} is observed at the phase transition temperature and for lipids in the liquid-crystalline phase subnanosecond τ_{rot} is observed [87,88]. Hence, we conclude that more bulky lipids, as present in the *E. coli* lipid mixtures, lead to smaller amplitudes of overall lipid motion as indicated by higher lipid order parameters, S^2_{lip}. At the same time typical characteristics of small, isotropic bicelles are maintained as indicated by translational diffusion data. Moreover, the small lipid correlation times observed in this study indicate that the bicelles are in a liquid-disordered phase at 25 °C.

In a direct comparison of either the dynamic parameters (Fig. 4, Table 3), or R_1 data directly (Fig. 5) it is clear that the lipids in all bicelles have very similar dynamics, irrespective of growth temperature or composition. As noted earlier, *E. coli* cells adapt the composition of their membranes such that a fluid, lamellar phase is maintained. The L_β to L_α phase transition occurs >10 °C below the growth temperature [90], while non-lamellar phases are observed approximately 20 °C above the growth temperature [11]. Since we do not observe any changes in the dynamics, we conclude that all three bicelle types are in a fluid, lamellar phase at 25 °C. The fact that an L_α phase is maintained by bacteria explains why it is possible to make bicelles of all native lipid extracts used here. In contrast, in our hands, it was not possible to produce bicelles of synthetic lipids having a lipid composition similar to AD93WT lipid extracts or with a charge density that exceeds 50% PG. A plausible explanation for this is that by adjusting its acyl chain composition *E. coli* maintains an L_α phase and this delicately balanced

acyl chain composition is not easily reproducible in vitro by using synthetic lipids.

5. Conclusions

In order to study protein-membrane interactions by solution-state NMR sufficiently small membrane mimetics that closely mimic natural membranes are required. Such systems can be constructed from native lipids purified from *E. coli* strains and the lipid and acyl chain composition can to some extent be tuned by the choice of growth temperature, growth phase, and bacterial strain. Lipids in fast-tumbling bicelles exhibit a broad range of ps–ns dynamics ranging from the rigid glycerol backbone to the nearly unrestricted motions of methyl groups at the end of acyl chains. Our results demonstrate that the lipids in these bicelles have dynamic properties on the ps–ns time-scale that match those found in other systems, and therefore provide a good mimetic of the bacterial lipid bilayer. Acyl chain modifications locally modify the $^{1}H—_{13}C$ bond dynamics. Fast-tumbling bicelles produced in this way, with an original lipid composition of bacterial membranes, will therefore prove useful for studying the membrane interacting properties of bacterial proteins and peptides. Moreover, bicelles constructed from lipids of a strain that does not synthesize PE, the most abundant lipid in *E. coli*, will allow studying the specific role of PE for such interactions.

Transparency document

The Transparency document associated with this article can be found, in online version.

Acknowledgements

This work was supported by grants from the Swedish Research Council (contract number 621-2014-3706) and by a grant from the Carl Trygger Foundation for Scientific Research (Grant number CTS 13:311). The Knut and Alice Wallenberg Foundation is acknowledged for NMR spectrometer support.

Appendix A. Supplementary data

Supplementary data to this article can be found online at http://dx.doi.org/10.1016/j.bbamem.2016.06.008.

References

[1] J.E. Cronan, Bacterial membrane lipids: where do we stand? Annu. Rev. Microbiol. 57 (2003) 203–224.
[2] W. Dowhan, M. Bogdanov, Functional Roles of Lipids in Membranes, in: D.E. Vance, J.E. Vance (Eds.), Biochemistry of Lipids, Lipoproteins and Membranes, Vol. 36, Elsevier, Amsterdam 2002, pp. 1–35.
[3] M. Bogdanov, P.N. Heacock, W. Dowhan, A polytopic membrane protein displays a reversible topology dependent on membrane lipid composition, EMBO J. 21 (2002) 2107–2116.
[4] L. Lindholm, C. Ariöz, M. Jawurek, J. Liebau, L. Mäler, Å. Wieslander, C. von Ballmoos, A. Barth, Effect of lipid bilayer properties on the photocycle of green proteorhodopsin, Biochim. Biophys. Acta 1847 (2015) 698–708.
[5] L. Li, P. Storm, O.P. Karlsson, S. Berg, Å. Wieslander, Irreversible binding and activity control of the 1,2-diacylglycerol 3-glucosyltransferase from *Acholeplasma laidlawii* at an anionic lipid bilayer surface, Biochemistry 42 (2003) 9677–9686.
[6] J. Lind, T. Rämö, M.L. Klement, E. Barany-Wallje, R.M. Epand, R.F. Epand, L. Mäler, Å. Wieslander, High cationic charge and bilayer interface-binding helices in a regulatory lipid glycosyltransferase, Biochemistry 46 (2007) 5664–5677.
[7] C. Ariöz, W. Ye, A. Bakali, C. Ge, J. Liebau, H. Götzke, A. Barth, Å. Wieslander, L. Mäler, Anionic lipid binding to the foreign protein MGS provides a tight coupling between phospholipid synthesis and protein overexpression in *Escherichia coli*, Biochemistry 52 (2013) 5533–5544.
[8] J. Liebau, P. Pettersson, S. Szpryngiel, L. Mäler, Membrane interaction of the glycosyltransferase WaaG, Biophys. J. 109 (2015) 552–563.
[9] A. Shokri, G. Larsson, Characterisation of the *Escherichia coli* membrane structure and function during fedbatch cultivation, Microb. Cell Factories 3 (2004) 9.
[10] M. Luckey, Membrane Structural Biology, Cambridge University Press, New York, 2008.
[11] S. Morein, A. Andersson, L. Rilfors, G. Lindblom, Wild-type *Escherichia coli* cells regulate the membrane lipid composition in a "window" between gel and non-lamellar structures, J. Biol. Chem. 271 (1996) 6801–6809.
[12] W. Dowhan, Molecular basis for membrane phospholipid diversity: why are there so many lipids? Annu. Rev. Biochem. 66 (1997) 199–232.
[13] S. Hiraoka, H. Matsuzaki, I. Shibuya, Active increase in cardiolipin synthesis in the stationary growth phase and its physiological significance in *Escherichia coli*, FEBS Lett. 336 (1993) 221–224.
[14] A.G. Marr, J.L. Ingraham, Effect of temperature on the composition of fatty acids in *Escherichia coli*, J. Bacteriol. 84 (1962) 1260–1267.
[15] M. Wikström, A.A. Kelly, A. Georgiev, H.M. Eriksson, M.R. Klement, M. Bogdanov, W. Dowhan, Å. Wieslander, Lipid-engineered *Escherichia coli* membranes reveal critical lipid headgroup size for protein function, J. Biol. Chem. 284 (2009) 954–965.
[16] D.W. Grogan, J.E. Cronan Jr., Cyclopropane ring formation in membrane lipids of bacteria, Microbiol. Mol. Biol. Rev. 61 (1997) 429–441.
[17] D. Poger, A.E. Mark, A ring to rule them all: the effect of cyclopropane fatty acids on the fluidity of lipid bilayers, J. Phys. Chem. B 119 (2015) 5487–5495.
[18] A. Wang, J.E. Cronan, The growth phase-dependent synthesis of cyclopropane fatty acids in *Escherichia coli* is the result of an RpoS (KatF)-dependent promoter plus enzyme instability, Mol. Microbiol. 11 (1994) 1009–1017.
[19] I. Vasilenko, B. De Kruijff, A.J. Verkleij, Polymorphic phase behaviour of cardiolipin from bovine heart and from *Bacillus subtilis* as detected by 31P NMR and freeze-fracture techniques. Effects of Ca^{2+}, Mg^{2+}, Ba^{2+} and temperature, Biochim. Biophys. Acta 684 (1982) 282–286.
[20] D.E. Warschawski, Membrane proteins of known structure determined by NMR, http://www.drorlist.com/nmr/MPNMR.html13 Jan 2016.
[21] D.E. Warschawski, A.A. Arnold, M. Beaugrand, A. Gravel, E. Chartrand, I. Marcotte, Choosing membrane mimetics for NMR structural studies of transmembrane proteins, Biochim. Biophys. Acta 1808 (2011) 1957–1974.
[22] P.J. Booth, M.L. Riley, S.L. Flitsch, R.H. Templer, A. Farooq, A.R. Curran, N. Chadborn, P. Wright, Evidence that bilayer bending rigidity affects membrane protein folding, Biochemistry 36 (1997) 197–203.
[23] J.J. Chou, J.D. Kaufman, S.J. Stahl, P.T. Wingfield, A. Bax, Micelle-induced curvature in a water-insoluble HIV-1 Env peptide revealed by NMR dipolar coupling measurement in stretched polyacrylamide gel, J. Am. Chem. Soc. 124 (2002) 2450–2451.
[24] L. Cristian, J.D. Lear, W.F. DeGrado, Use of thiol-disulfide equilibria to measure the energetics of assembly of transmembrane helices in phospholipid bilayers, Proc. Natl. Acad. Sci. U. S. A. 100 (2003) 14772–14777.
[25] S.B. Long, X. Tao, E.B. Campbell, R. MacKinnon, Atomic structure of a voltage-dependent K^{+} channel in a lipid membrane-like environment, Nature 450 (2007) 376–382.
[26] T.L. Lau, A.W. Partridge, M.H. Ginsberg, T.S. Ulmer, Structure of the integrin β3 transmembrane segment in phospholipid bicelles and detergent micelles, Biochemistry 47 (2008) 4008–4016.
[27] M. Sharma, M. Yi, H. Dong, H. Qin, E. Peterson, D.D. Busath, H.X. Zhou, T.A. Cross, Insight into the mechanism of the influenza A proton channel from a structure in a lipid bilayer, Science 330 (2010) 509–512.
[28] T.A. Cross, M. Sharma, M. Yi, H.X. Zhou, Influence of solubilizing environments on membrane protein structures, Trends Biochem. Sci. 36 (2011) 117–125.
[29] I. Marcotte, M. Auger, Bicelles as model membranes for solid- and solution-state NMR studies of membrane peptides and proteins, Concept Magn. Reson. A 24 (2005) 17–37.
[30] J. Liebau, Y. Weihua, L. Mäler, Characterization of fast-tumbling isotropic bicelles by PFG diffusion NMR, Magn. Reson. Chem. (2015), http://dx.doi.org/10.1002/mrc.4399.
[31] J.J. Chou, J.L. Baber, A. Bax, Characterization of phospholipid mixed micelles by translational diffusion, J. Biomol. NMR 29 (2004) 299–308.
[32] L. Mäler, Solution NMR studies of peptide-lipid interactions in model membranes, Mol. Membr. Biol. 29 (2012) 155–176.
[33] S. Gaemers, A. Bax, Morphology of three lyotropic liquid crystalline biological NMR media studied by translational diffusion anisotropy, J. Am. Chem. Soc. 123 (2001) 12343–12352.
[34] M. Nieh, C.J. Glinka, S. Krueger, S.R. Prosser, J. Katsaras, SANS study of the structural phases of magnetically alignable lanthanide-doped phospholipid mixtures, Langmuir 17 (2001) 2629–2638.
[35] M. Beaugrand, A.A. Arnold, J. Henin, D.E. Warschawski, P.T. Williamson, I. Marcotte, Lipid concentration and molar ratio boundaries for the use of isotropic bicelles, Langmuir 30 (2014) 6162–6170.
[36] C.R. Sanders, R.S. Prosser, Bicelles: a model membrane system for all seasons? Structure 6 (1998) 1227–1234.
[37] R.R. Vold, R.S. Prosser, A.J. Deese, Isotropic solutions of phospholipid bicelles: a new membrane mimetic for high-resolution NMR studies of polypeptides, J. Biomol. NMR 9 (1997) 329–335.
[38] A. Andersson, L. Mäler, NMR solution structure and dynamics of motilin in isotropic phospholipid bicellar solution, J. Biomol. NMR 24 (2002) 103–112.
[39] E. Barany-Wallje, A. Andersson, A. Gräslund, L. Mäler, Dynamics of transportan in bicelles is surface charge dependent, J. Biomol. NMR 35 (2006) 137–147.
[40] I. Marcotte, F. Separovic, M. Auger, S.M. Gagne, A multidimensional 1H NMR investigation of the conformation of methionine-enkephalin in fast-tumbling bicelles, Biophys. J. 86 (2004) 1587–1600.
[41] J. Wang, J.R. Schnell, J.J. Chou, Amantadine partition and localization in phospholipid membrane: a solution NMR study, Biochem. Biophys. Res. Commun. 324 (2004) 212–217.
[42] J. Struppe, J.A. Whiles, R.R. Vold, Acidic phospholipid bicelles: a versatile model membrane system, Biophys. J. 78 (2000) 281–289.

[43] W. Ye, J. Liebau, L. Mäler, New membrane mimetics with galactolipids: lipid properties in fast-tumbling bicelles, J. Phys. Chem. B 117 (2013) 1044–1050.
[44] J. Lind, J. Nordin, L. Mäler, Lipid dynamics in fast-tumbling bicelles with varying bilayer thickness: effect of model transmembrane peptides, Biochim. Biophys. Acta 1778 (2008) 2526–2534.
[45] M.N. Triba, P.F. Devaux, D.E. Warschawski, Effects of lipid chain length and unsaturation on bicelles stability. A phosphorus NMR study, Biophys. J. 91 (2006) 1357–1367.
[46] A. Andersson, L. Mäler, Motilin-bicelle interactions: membrane position and translational diffusion, FEBS Lett. 545 (2003) 139–143.
[47] J.L. Markley, A. Bax, Y. Arata, C. Hilbers, R. Kaptein, B.D. Sykes, P.E. Wright, K. Wüthrich, Recommendations for the presentation of NMR structures of proteins and nucleic acids, J. Mol. Biol. 280 (1998) 933–952.
[48] W.W. Christie, A.J. Dijkstra, G. Knothe, Analysis, in: J.L. Harwood, F.D. Gunstone, A.J. Dijkstra (Eds.), The Lipid Handbook with CD-ROM, third ed.CRC Press, Boca Raton 2007, pp. 415–469.
[49] D.Y. Sze, O. Jardetzky, Characterization of lipid composition in stimulated human lymphocytes by 1H NMR, Biochim. Biophys. Acta 1054 (1990) 198–206.
[50] P. Meneses, T. Glonek, High resolution 31P NMR of extracted phospholipids, J. Lipid Res. 29 (1988) 679–689.
[51] R. Karlicek, I. Lowe, A modified pulsed gradient technique for measuring diffusion in the presence of large background gradients, J. Magn. Reson. 37 (1980) 75–91.
[52] D.H. Wu, A.D. Chen, C.S. Johnson, An improved diffusion-ordered spectroscopy experiment incorporating bipolar-gradient pulses, J. Magn. Reson. Ser. A 115 (1995) 260–264.
[53] W.H. Otto, C.K. Larive, Improved spin-echo-edited NMR diffusion measurements, J. Magn. Reson. 153 (2001) 273–276.
[54] E.O. Stejskal, J.E. Tanner, Spin diffusion measurements: spin echoes in the presence of a time-dependent field gradient, J. Chem. Phys. 42 (1965) 288–292.
[55] L.G. Longsworth, The mutual diffusion of light and heavy water, J. Phys. Chem. 64 (1960) 1914–1917.
[56] H. Wennerström, G. Lindblom, B. Lindman, Theoretical aspects on NMR of quadrupolar ionic nuclei in micellar solutions and amphiphilic liquid-crystals, Chem. Scr. 6 (1974) 97–103.
[57] H. Wennerström, B. Lindman, O. Söderman, T. Drakenberg, J.B. Rosenholm, 13C magnetic relaxation in micellar solutions. Influence of aggregate motion on T_1, J. Am. Chem. Soc. 101 (1979) 6860–6864.
[58] B. Halle, H. Wennerström, Interpretation of magnetic resonance data from water nuclei in heterogeneous systems, J. Chem. Phys. 75 (1981) 1928–1943.
[59] G. Lipari, A. Szabo, Model-free approach to the interpretation of nuclear magnetic resonance relaxation in macromolecules. 1. Theory and range of validity, J. Am. Chem. Soc. 104 (1982) 4546–4559.
[60] G. Lipari, A. Szabo, Model-free approach to the interpretation of nuclear magnetic relaxation in macromolecules. 2. Analysis of experimental results, J. Am. Chem. Soc. 104 (1982) 4559–4570.
[61] M.F. Brown, A.A. Ribeiro, G.D. Williams, New view of lipid bilayer dynamics from 2H and 13C NMR relaxation time measurements, Proc. Natl. Acad. Sci. U. S. A. 80 (1983) 4325–4329.
[62] J.F. Ellena, L.S. Lepore, D.S. Cafiso, Estimating lipid lateral diffusion in phospholipid vesicles from carbon-13 spin-spin relaxation, J. Phys. Chem. 97 (1993) 2952–2957.
[63] J. Kowalewski, L. Mäler, Nuclear Spin Relaxation in Liquids; Theory, Experiments, and Applications, CRC Press, Boca Raton, 2006.
[64] A.G. Palmer III, NMR probes of molecular dynamics: overview and comparison with other techniques, Annu. Rev. Biophys. Biomol. Struct. 30 (2001) 129–155.
[65] J. Björnerås, M. Nilsson, L. Mäler, Analysing DHPC/DMPC bicelles by diffusion NMR and multivariate decomposition, Biochim. Biophys. Acta 1848 (2015) 2910–2917.
[66] A.W. Draney, S.T. Smrt, J.L. Lorieau, Use of isotropically tumbling bicelles to measure curvature induced by membrane components, Langmuir 30 (2014) 11723–11733.
[67] S. Unnerståle, L. Mäler, R.R. Draheim, Structural characterization of AS1-membrane interactions from a subset of HAMP domains, Biochim. Biophys. Acta 1808 (2011) 2403–2412.
[68] D. de Mendoza, J.E. Cronan, Thermal regulation of membrane lipid fluidity in bacteria, Trends Biochem. Sci. 8 (1983) 49–52.
[69] Y.Y. Chen, M.G. Gänzle, Influence of cyclopropane fatty acids on heat, high pressure, acid and oxidative resistance in *Escherichia coli*, Int. J. Food Microbiol. 222 (2016) 16–22.
[70] D. Charoenwong, S. Andrews, B. Mackey, Role of rpoS in the development of cell envelope resilience and pressure resistance in stationary-phase *Escherichia coli*, Appl. Environ. Microbiol. 77 (2011) 5220–5229.
[71] M.A. Casadei, P. Manas, G. Niven, E. Needs, B.M. Mackey, Role of membrane fluidity in pressure resistance of *Escherichia coli* NCTC 8164, Appl. Environ. Microbiol. 68 (2002) 5965–5972.
[72] H. Asakura, T. Ekawa, N. Sugimoto, Y. Momose, K. Kawamoto, S. Makino, S. Igimi, S. Yamamoto, Membrane topology of *Salmonella* invasion protein SipB confers osmotolerance, Biochem. Biophys. Res. Commun. 426 (2012) 654–658.
[73] A. Guillot, D. Obis, M. Mistou, Fatty acid membrane composition and activation of glycine-betaine transport in *Lactococcus lactis* subjected to osmotic stress, Int. J. Food Microbiol. 55 (2000) 47–51.
[74] Y. Chang, J.E. Cronan, Membrane cyclopropane fatty acid content is a major factor in acid resistance of *Escherichia coli*, Mol. Microbiol. 33 (1999) 249–259.
[75] S. Nishijima, Y. Asami, N. Uetake, S. Yamagoe, A. Ohta, I. Shibuya, Disruption of the *Escherichia coli* cls gene responsible for cardiolipin synthesis, J. Bacteriol. 170 (1988) 775–780.
[76] I. Shibuya, C. Miyazaki, A. Ohta, Alteration of phospholipid composition by combined defects in phosphatidylserine and cardiolipin synthases and physiological consequences in *Escherichia coli*, J. Bacteriol. 161 (1985) 1086–1092.
[77] B.E. Tropp, Cardiolipin synthase from *Escherichia coli*, Biochim. Biophys. Acta 1348 (1997) 192–200.
[78] P. Bernal, J. Muñoz-Rojas, A. Hurtado, J.L. Ramos, A. Segura, A *Pseudomonas putida* cardiolipin synthesis mutant exhibits increased sensitivity to drugs related to transport functionality, Environ. Microbiol. 9 (2007) 1135–1145.
[79] Y. Zhang, C.O. Rock, Membrane lipid homeostasis in bacteria, Nat. Rev. Microbiol. 6 (2008) 222–233.
[80] T. Romantsov, Z. Guan, J.M. Wood, Cardiolipin and the osmotic stress responses of bacteria, Biochim. Biophys. Acta 1788 (2009) 2092–2100.
[81] E. Mileykovskaya, W. Dowhan, Cardiolipin membrane domains in prokaryotes and eukaryotes, Biochim. Biophys. Acta 1788 (2009) 2084–2091.
[82] R. Arias-Cartin, S. Grimaldi, P. Arnoux, B. Guigliarelli, A. Magalon, Cardiolipin binding in bacterial respiratory complexes: structural and functional implications, Biochim. Biophys. Acta 1817 (2012) 1937–1949.
[83] J.E. Cronan Jr., Phospholipid alterations during growth of *Escherichia coli*, J. Bacteriol. 95 (1968) 2054–2061.
[84] A. DeChavigny, P.N. Heacock, W. Dowhan, Sequence and inactivation of the pss gene of *Escherichia coli*. Phosphatidylethanolamine may not be essential for cell viability, J. Biol. Chem. 266 (1991) 5323–5332.
[85] L.S. Lepore, J.F. Ellena, D.S. Cafiso, Comparison of the lipid acyl chain dynamics between small and large unilamellar vesicles, Biophys. J. 61 (1992) 767–775.
[86] A. Andersson, L. Mäler, Magnetic resonance investigations of lipid motion in isotropic bicelles, Langmuir 21 (2005) 7702–7709.
[87] H.S. Camargos, A. Alonso, Electron paramagnetic resonance (EPR) spectral components of spin-labeled lipids in saturated phospholipid bilayers: effect of cholesterol, Quim. Nova 36 (2013) 815–821.
[88] D. Marsh, Molecular motion in phospholipid bilayers in the gel phase: long axis rotation, Biochemistry 19 (1980) 1632–1637.
[89] O.H. Griffith, P.C. Jost, Lipid Spin Labels in Biological Membranes, in: L.J. Berliner (Ed.), Spin Labeling: Theory and Applications, Vol. 1, Academic Press, New York 1976, pp. 453–524.
[90] M.B. Jackson, J.E. Cronan Jr., An estimate of the minimum amount of fluid lipid required for the growth of *Escherichia coli*, Biochim. Biophys. Acta 512 (1978) 472–479.